

**Reduced thermal conductivity of hydrous aluminous silica and calcium ferrite-type phase promote water transportation to Earth's deep mantle**

**Wen-Pin Hsieh<sup>1,2\*</sup>, Takayuki Ishii<sup>3</sup>, Frédéric Deschamps<sup>1</sup>, Yi-Chi Tsao<sup>1</sup>, Jen-Wei Chang<sup>1</sup>, and Giacomo Criniti<sup>4</sup>**

<sup>1</sup>Institute of Earth Sciences, Academia Sinica, Taipei 11529, Taiwan

<sup>2</sup>Department of Geosciences, National Taiwan University, Taipei 10617, Taiwan

<sup>3</sup>Institute for Planetary Materials, Okayama University, 827 Yamada, Misasa, Tottori 682-0193, Japan

<sup>4</sup>Earth and Planets Laboratory, Carnegie Institution for Science, Washington, DC, USA

Corresponding author: Wen-Pin Hsieh ([wphsieh@earth.sinica.edu.tw](mailto:wphsieh@earth.sinica.edu.tw))

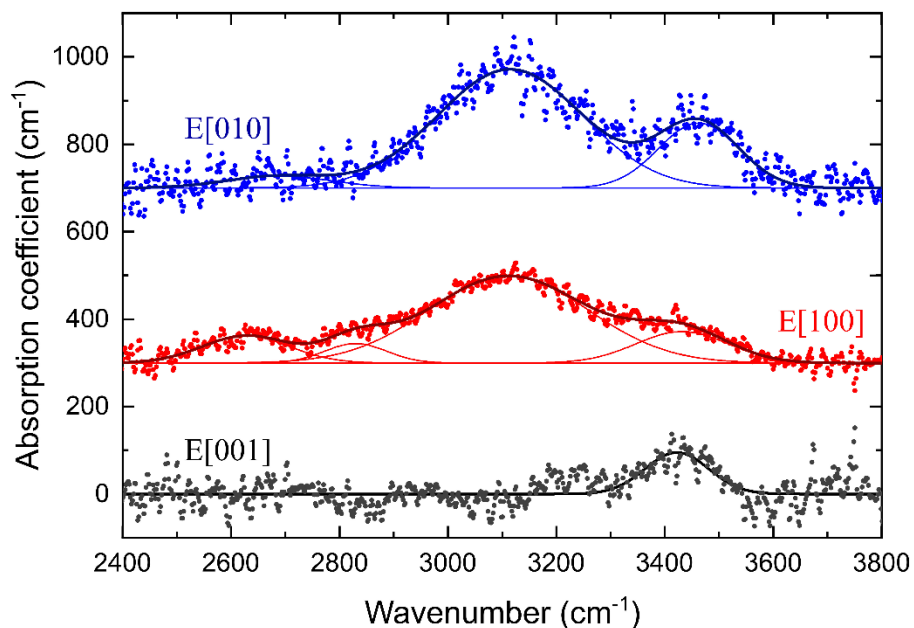
**Contents of this file**

Figures S1 to S4  
Table S1

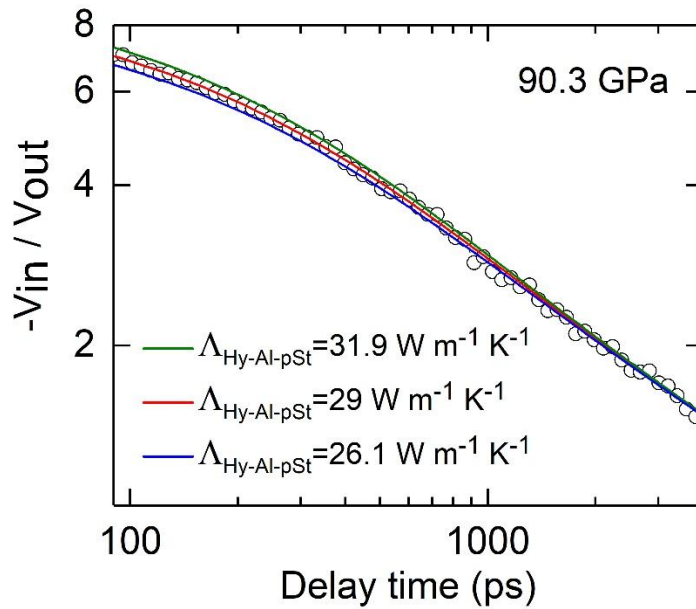
**Introduction**

There are four figures and one table that show supporting information to the present study. Figure S1 plots the polarized Fourier transform infrared (FT-IR) spectra for hydrous aluminous post-stishovite. Figure S2 shows a set of raw TDTR spectrum fitted by the thermal model. Figure S3 presents analysis of data uncertainty caused by uncertainty of each model parameter. Table S1 lists a set of input parameters used in the thermal model

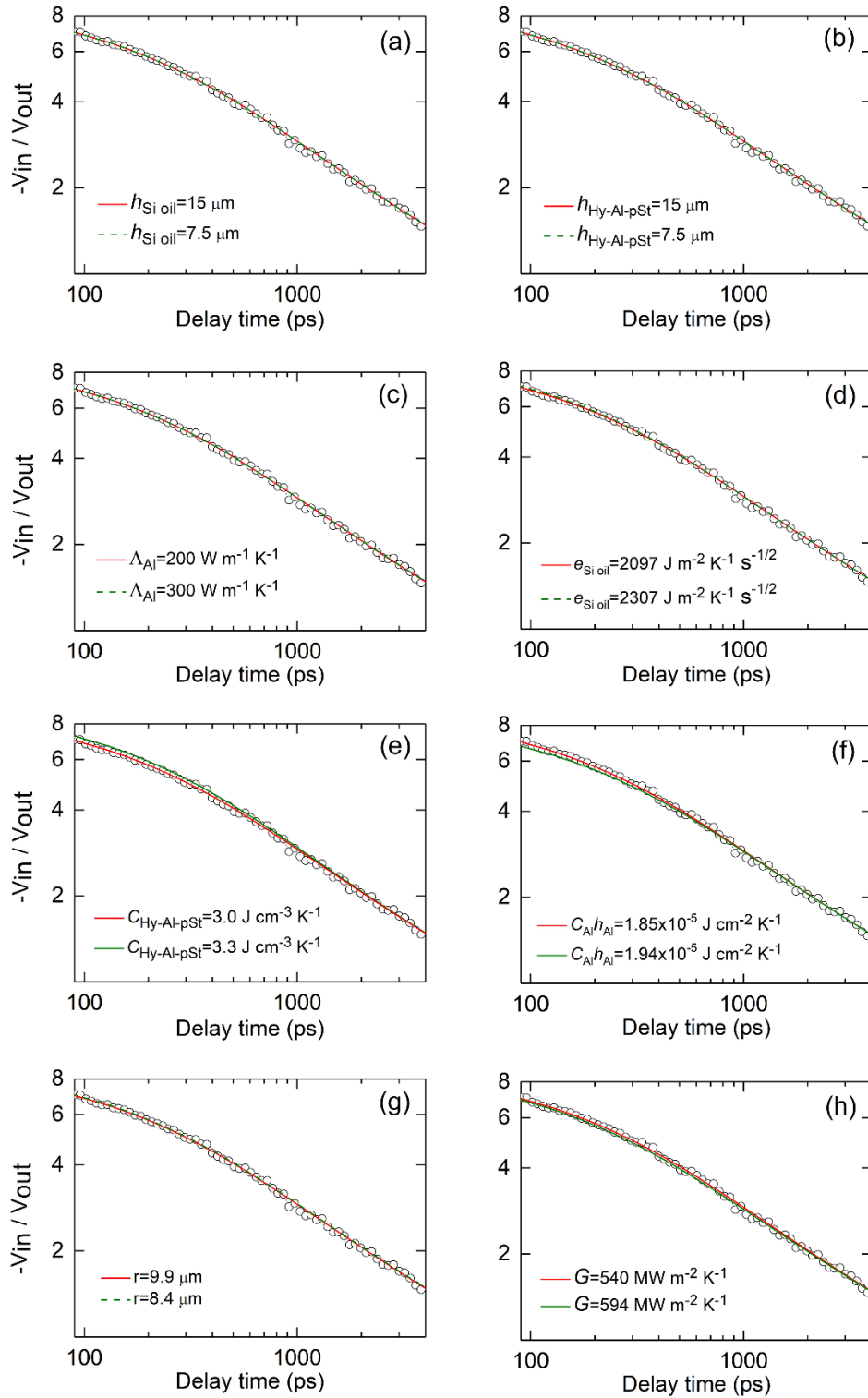
for hydrous aluminous post-stishovite at 90.3 GPa and 300 K. Figure S4 shows the Raman spectrum of hydrous aluminous post-stishovite at high pressures.



**Supplementary Figure S1.** Example polarized Fourier transform infrared (FT-IR) spectra for hydrous aluminous post-stishovite at ambient conditions oriented along the (010) and (100) crystallographic planes, respectively, as indicated in the top two sub-plots. The spectrum along (001) at the bottom was plotted for comparison.

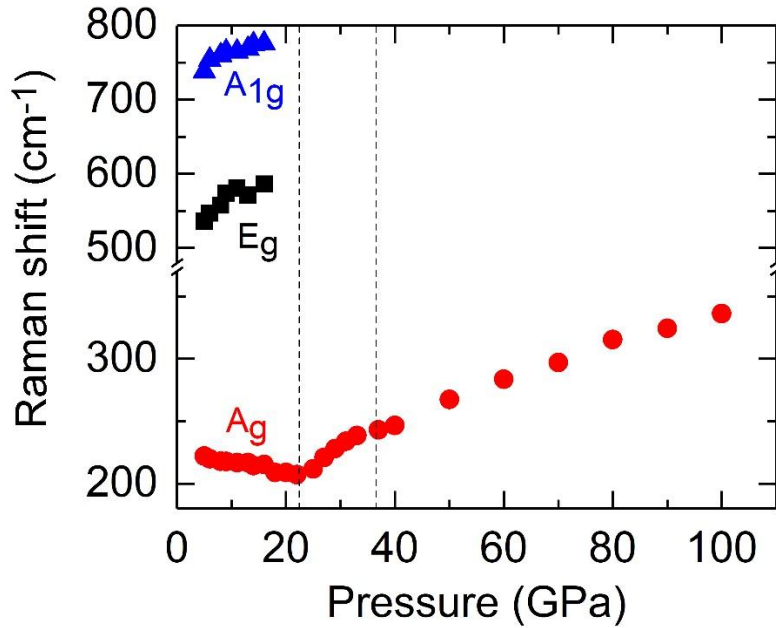


**Supplementary Figure S2.** Representative TDTR data (open circles) for hydrous aluminous pSt (Hy-Al-pSt) at 90.3 GPa and room temperature fitted by thermal model simulations (color solid curves). The raw TDTR data is best-fitted with  $\Lambda_{\text{Hy-Al-pSt}} = 29 \text{ W m}^{-1} \text{ K}^{-1}$  (red curve) using a set of input parameters listed in Supplementary Table S1. The data for  $-V_{in}/V_{out}$  is most sensitive to the sample's thermal conductivity at delay time of few hundred picosecond (ps), see (Cahill & Watanabe, 2004; Zheng et al., 2007) for details. When fitting the data with a  $\Lambda_{\text{Hy-Al-pSt}}$  that is 10% difference (green and blue curves) than the best-fitted  $\Lambda_{\text{Hy-Al-pSt}} = 29 \text{ W m}^{-1} \text{ K}^{-1}$ , the thermal model simulation yields a poor fitting, which indicates that our data analysis is highly sensitive and precise due to our high-quality data.



**Supplementary Figure S3.** Sensitivity tests of the thermal model simulation to several key input parameters for hydrous aluminous pSt (Hy-Al-pSt) at 90.3 GPa. Here we fix the thermal conductivity of Hy-Al-pSt,  $\Lambda_{\text{Hy-Al-pSt}}$ , at  $29 \text{ W m}^{-1} \text{ K}^{-1}$  as derived in Supplementary Fig. S2. (a) and (b) The model simulations remain essentially the same, even if the

thicknesses of the pressure medium silicone oil ( $h_{\text{Si oil}}$ ) and Hy-Al-pSt sample ( $h_{\text{Hy-Al-pSt}}$ ) are changed by 50%, respectively. These indicate that their individual uncertainty does not affect the  $\Lambda_{\text{Hy-Al-pSt}}$ . **(c)** Again, the model simulation remains the same even if the high thermal conductivity of Al film increases at high pressures, i.e., its uncertainty has no effect on the  $\Lambda_{\text{Hy-Al-pSt}}$ . **(d)** If there is an example 10% uncertainty from the thermal effusivity of the pressure medium silicone oil,  $e=(\Lambda_{\text{Si}}C_{\text{Si}})^{1/2}$ , the model simulation is hardly changed, i.e., its uncertainty has very minor effect on the  $\Lambda_{\text{Hy-Al-pSt}}$ . **(e)** If there is a 10% uncertainty in the volumetric heat capacity of Hy-Al-pSt,  $C_{\text{Hy-Al-pSt}}$ , the data can be re-fitted by a slightly lower  $\Lambda_{\text{Hy-Al-pSt}}=27 \text{ W m}^{-1} \text{ K}^{-1}$ , i.e., minorly propagating  $\sim 7\%$  uncertainty. **(f)** The uncertainty in the heat capacity of Al film per unit area (product of Al's volumetric heat capacity and thickness,  $C_{\text{Al}} h_{\text{Al}}$ , see (Zheng et al., 2007)) is the major uncertainty of our data analysis. If there is an example 5% uncertainty, a slightly higher  $\Lambda_{\text{Hy-Al-pSt}}=31 \text{ W m}^{-1} \text{ K}^{-1}$  ( $\sim 6.8\%$  change) re-fits well the data. **(g)** A 15% uncertainty in the laser spot size and **(h)** a 10% off in the thermal conductance of Hy-Al-pSt and Al/silicone oil interfaces,  $G$ , respectively, does not significantly influence the model simulations. These results indicate that their uncertainties have very little effect on the  $\Lambda_{\text{Hy-Al-pSt}}$ .



**Supplementary Figure S4.** Raman shift of the Hy-Al-pSt as a function of pressure. The characteristic  $A_g$  mode at  $\sim 230 \text{ cm}^{-1}$  softens with initial compression, while its pressure slope becomes small around 22 GPa, after which the frequency increases with higher pressure.

**Supplementary Table S1.** Input parameters in the thermal model for Hy-Al-pSt at 90.3

GPa and 300 K in TDTR measurements

$P$ (GPa)	$C_{\text{Hy-Al-pSt}}$ ( $\text{J cm}^{-3} \text{ K}^{-1}$ )	$C_{\text{Al}}$ ( $\text{J cm}^{-3} \text{ K}^{-1}$ )	$h_{\text{Al}}$ (nm)*	$e=(\Lambda_{\text{Si}}C_{\text{Si}})^{1/2}$ ( $\text{J m}^{-2} \text{ K}^{-1} \text{ s}^{-1/2}$ )	$r$ ( $\mu\text{m}$ )	$h_{\text{Hy-Al-pSt/Si oil}}$ ( $\mu\text{m}$ )	$\Lambda_{\text{Al}}$ ( $\text{W m}^{-1} \text{ K}^{-1}$ )	$G$ ( $\text{MW m}^{-2} \text{ K}^{-1}$ )
90.3	3	2.683	69.0	2097	9.9	15/15	200	540

\*In this experimental run, the Al thickness at ambient pressure is 88.2 nm.

$C_{\text{Hy-Al-pSt}}$ : Hy-Al-pSt heat capacity,  $C_{\text{Al}}$ : Al heat capacity,  $h_{\text{Al}}$ : Al thickness,  $e$ : silicone oil thermal effusivity,  $r$ : laser spot size,  $h_{\text{Hy-Al-pSt}}$ : Hy-Al-pSt thickness,  $h_{\text{Si oil}}$ : silicone oil thickness,  $\Lambda_{\text{Al}}$ : Al thermal conductivity,  $G$ : thermal conductance of Al/Hy-Al-pSt and Al/silicone oil interfaces.

## Supplementary References

- Cahill, D. G., & Watanabe, F. (2004). Thermal conductivity of isotopically pure and Ge-doped Si epitaxial layers from 300 to 550 K. *Phys. Rev. B*, 70(23), 235322.  
<https://doi.org/10.1103/PhysRevB.70.235322>
- Zheng, X., Cahill, D. G., Krasnochtchekov, P., Averbach, R. S., & Zhao, J. C. (2007). High-throughput thermal conductivity measurements of nickel solid solutions and the applicability of the Wiedemann-Franz law. *Acta Materialia*, 55(15), 5177–5185.  
<https://doi.org/10.1016/j.actamat.2007.05.037>